IJBPAS, January, 2025, 14(1): 40-60

ISSN: 2277–4998

International Journal of Biology, Pharmacy and Allied Sciences (IJBPAS)

'A Bridge Between Laboratory and Reader'

www.ijbpas.com

ENHANCED BIOAVAILABILITY OF ANTIARTHRITIC DRUGS BY HERBAL INHIBITORS OF P-GLYCOPROTEIN – *IN SILICO* APPROACH

ROY C[1], ROY S[2], GANGULI S[3] AND GHOSH P[4*]

1: Department of Physiology, West Bengal State University, Kolkata-700126, India, ORCiD : https://orcid.org/0000-0003-3294-894X

2: Department of Biotechnology, Rajalakshmi Engineering College, Chennai-602105, India, ORCiD: https://orcid.org/0000-0002-5203-2050

3: Post Graduate and Research Department of Biotechnology, St. Xavier's College (Autonomous), Kolkata-700016, India, ORCiD: https://orcid.org/0000-0001-5481-7436

4: Department of Physiology, West Bengal State University, Kolkata-700126, India, ORCiD: https://orcid.org/0000-0002-9194-2882

***Corresponding Author: Dr. Pratiti Ghosh: E Mail: pratitig@wbsu.ac.in**

Received 24th Sept. 2023; Revised 25th Oct. 2023; Accepted 25th March 2024; Available online 1st Jan. 2025

https://doi.org/10.31032/IJBPAS/2025/14.1.8478

ABSTRACT

Background: P-glycoprotein is an efflux transporter implicated in drug resistance in arthritic patients. Coadministration of medicinal herbal components as inhibitors may configure the transporter in favour of the drug, thus curtailing its expulsion. **Objective:** This study endeavours to analyze the components of antiarthritic herbs in inhibition of p-glycoprotein receptor thus enhancing the possibility of retention of coadministered antiarthritic medications in the cell. **Methods:** Druggability and pharmacokinetic profile of the compounds were examined. Cluster analysis of p-glycoprotein inhibitors was performed with ChemMine based on structural similarities and physicochemical properties. Molecular docking utilizing Discovery Studio, was performed to interpret the maximum binding affinity between 22 inhibitory compounds and the receptor (6C0V). **Results:** The docking analyses revealed that the inhibitors viz., thionuphlutine B (*Nuphar pumilum)*, kihadanin A (*Phellodendron amurense)* and kopsamine (*Kopsia arborea)* bind with -187.15, -150.85 and -126.20 (Kcal/mol) energy, respectively. **Conclusion:** Molecular dynamics simulation validated the stability of the receptor-

thionuphlutine B complex, which may thus be recognized as the lead compound in augmentation of drug bioavailability inside the cell, along with its herbal antiarthritic therapeutic efficacy.

Keywords : antiarthritic, docking, inhibitors, medicinal herbs, p-glycoprotein

INTRODUCTION

Human p-glycoprotein is an adenosine triphosphate (ATP)-dependent efflux transporter that has been associated with drug resistance in arthritic patients due to its defensive property of extrusion of intracellular drugs **[1]**. This glycoprotein is located on the long arm of chromosome 7(7q21) and comprises of two transmembrane domains, each constituting six putative alpha helices, two nucleotide-binding domains, all of which constitute the channel for substrate translocation across membrane **[2]**. Human p-glycoprotein is highly expressed in the capillary endothelial cells of blood–brain barrier, gastrointestinal tract, proximal convoluted tubular cells of kidney, liver, pancreas, heart, lungs, spleen, skeletal muscle etc. where it functions as a physiological barrier against the entry of xenobiotics into the body **[3]**. Its overexpression in lymphocytes during rheumatoid arthritis (RA) is associated with active efflux of corticosteroids and disease-modifying antirheumatic drugs (DMARDs), which are substrates of p-glycoprotein, thus culminating in reduced drug efficacy or drug resistance **[4]**. The peripheral blood lymphocytes from RA patients with highly active disease (Disease Activity Score (DAS) 28-3>5.1) was analyzed to elucidate the relationship between expression of p-glycoprotein and efflux of intracellular drugs. The intracellular and extracellular concentrations of dexamethasone (substrate of p-glycoprotein) were determined by the C/M ratio. The lymphocytes overexpressing p-glycoprotein showed low intracellular dexamethasone levels compared with those from RA patients with DAS 28-3<5.1 **[5]**. Inhibition of the transport function of p-glycoprotein could revert such drug resistance and improve bioavailability of the orally administered drugs in the target cell. Medicinal plants with plethora of bioactive components, have tissue regenerative characteristics and function in regulating inflammation in osteoarthritis **[6]**. These phytochemicals possess functional scaffolds to reverse p-glycoprotein mediated multidrug resistance **[7]**. The major antiarthritic drugs viz., baricitinib **[8]**; methotrexate **[9]**; prednisone **[10]**; apremilast **[11]**; tofacitinib **[12]**; cyclosporine **[13]** and upadacitinib **[14]** are substrates of p-glycoprotein and are hence effluxed by the cell.

So, twenty herbs with antiarthritic potency viz., *Cassia fistula, Hydnocarpus wightiana*, *Ficus bengalensis*, *Guaiacum officinale* **[15]**; *Artemisia japonica* **[16]**;

Nuphar pumilum **[17]**; *Justicia tranquebariensis* **[18]**; *Hypericum mysorense* [19]; *Sambucus ebulus* **[20]**; *Rabdosia rubescens* **[21]**; *Tanacetum parthenium* **[22]**; *Cynanchum paniculatum* **[23]**; *Epimedium grandiflorum* **[24]**; *Silybum marianum* **[25]**; *Kopsia arborea* **[26]**; *Phellodendron amurense* **[27]**; *Toona sinensis* **[28]**; *Peganum harmala* **[29]**; *Glycomis arborea* **[30]**; *Hedychium spicatum* **[31]** have been selected to screen their inhibitory binding potency of the efflux transporter by molecular docking.

This study was designed to identify medicinal herbal components as inhibitors of p-glycoprotein, thus increasing the accumulation of treatment oriented chemical allopathic drugs inside the cells.

MATERIALS AND METHODS

Protein preparation: The p-glycoprotein structure (PDB code: 6C0V) **[32]** was used to study molecular docking between the receptor and medicinal herbal components. The PDB file for p-glycoprotein was acquired from the Protein Data Bank (http://www.rcsb.org). Dogsitescorer server was employed for the identification of potential binding pockets and subpockets in the protein structure.

The 'prepare protein' protocol of Discovery Studio executed the following steps: cleaned the protein, side-chain conformations were optimized using the ChiRotor algorithm, water molecules were removed, missing loop regions were modelled based on SEQRES information and titratable residues were protonated using predicted pKs.

Ligand preparation: 3D structures and canonical smiles of 236 ligand molecules and control drug verapamil, were obtained for molecular docking from Pubchem (https://pubchem.ncbi.nlm.nih.gov/) and ChemSpider (http://www.chemspider.com/) database. The canonical SMILES were then translated into spatial data file format with the help of online SMILE translator (https://cactus.nci.nih.gov/translate/). The prepare/filter ligands protocol performed tasks such as removal of duplicates, computing isomers and tautomers and generated 3D conformations.

Drug Likeness and ADMET analyses

Druggability of the components was evaluated with Molinspiration tool (http://www.molinspiration.com).

Pharmacokinetic study was performed to examine the ADMET (Absorption, Distribution, Metabolism, Excretion and Toxicity) property of the small molecules (http://biosig.unimelb.edu.au/pkcsm/prediction).

Molecular Docking analyses

The receptor-ligand docking investigation was performed by CDOCKER module of Discovery Studio (version 2019-2021). CDOCKER is application of CHARMm based docking algorithm using a

rigid receptor. High-temperature molecular dynamics was employed to produce a set of ligand conformations. Random orientations of the conformations were generated by translating the center of the ligand to a specified location within the receptor active site and performing a series of random rotations. Each orientation was subjected to simulated annealing molecular dynamics. A final minimization of the ligand in the rigid receptor using non-softened potential was performed. A set of refined ligand poses for each bioactive component was generated and analyzed on the basis of lowest binding free energy, hydrogen bonds and hydrophobic interactions.

Molecular Dynamics Simulation

The entire process of simulation can be divided into three major steps:

A) Evaluation of input structure:

An important factor in molecular dynamics (MD) simulation is the accuracy of the input structure. MD simulations may become unstable or give unrealistic results if the input structure contains small errors. The initial structure checking page checks for the most common problems in MD simulation inputs, allowing the user to select possible solutions. When alternate models or multiple subunits are present in the incoming structure, structure checking can also be used to select which fragments of the system should be simulated.

Checking consists of choosing from a list of possible options:

- Model of the structure.
- The structure chain/s.
- Alternate locations for residues and atoms
- Non-consecutive residues and gaps in sequence.
- Atom clashes such as steric, alpha-carbon, polar donor, and acceptor, apolar, and ionic positive/negative.
- The improper chirality.
- Unusual cis conformation of the peptide bond.
- Disulphide bonds.

The complex employed for the analyses passed the major checkpoints of the evaluation scheme.

B) Simulation:

The protein was considered as a system of beads (Cα atoms) interacting through a discontinuous potential in a discrete molecular dynamic simulation **[33-37]**. Potentials were assumed to be constant outside of the discontinuities, assuming a ballistic regime for the particles (constant potential, constant velocity) under all circumstances except when they reached a potential discontinuity.

At this point, the conservation of the linear momentum, angular momentum, and total energy is imposed, which alters the velocities of the colliding particles. In this investigation, all collisions were taken to be

elastic since the particles were restricted to move within a configurational space where the potential energy remained constant and kinetic energy remained unchanged.

The interaction potentials have been described as infinite square wells, with particle-particle distances varying between d1 = (1 − σ)R0 and d2 = (1 + σ)R0, with R0 representing the distance in the native conformation and 2σ being the width of the square well. The MD-averaged conformation was used as the native conformation, as in Brownian molecular dynamics. In the native conformation, residue-residue interaction potentials were determined only for particles separated by less than a cutoff radius Rc. Rc value of 8 Å and σ value of 0.1 were utilized for nonconsecutive Cα particles, however a smaller well width (σ = 0.05) was chosen for consecutive pairs of residues to keep the Cα-Cα distances closer to the anticipated value of 3.8 Å. This description of the potential reproduced the shape of the wells generated by the distance-dependent pseudoharmonic model **[38]**.

C) Trajectory analyses:

Trajectory analyses was performed using GROMACs commands:

- G_rms tool from the Gromacs package (XTC trajectory format) was utilized for the calculation of root mean square deviation (RMSD) along the trajectory.
- G_rmsf, a Gromacs package function, calculated the average root mean square deviation for each residue along the trajectory (XTC trajectory format).
- G_rmsf from the Gromacs package (XTC trajectory format) computed B-factor value for each residue.

Clustering

ChemMine web tool was employed for analyzing and clustering small molecules by structural similarities and physicochemical properties **[39]**. The JOELib tool was used for calculation of 38 physicochemical descriptors for each small molecule (https://chemminetools.ucr.edu/tools/launch_job/Properties/). ChemMine tool provide facility for hierarchical clustering which builds agglomeratively a hierarchy of clusters based on pairwise compound similarities defined using the atom pair descriptors and Tanimoto coefficient.

RESULTS AND DISCUSSION

236 components of twenty antiarthritic herbs were initially screened on the basis of druggability and ADMET properties. The drug-likeness score of 236 components were tested through Lipinski's rule of five. 191 components showed drug-likeness properties whereas 45 components failed in Lipinski's rule of five. ADMET predictions were designed to evaluate the pharmacokinetic and toxicity properties. Analysis of pkcsm results revealed that 22 of 191 components, serve as p-glycoprotein

inhibitors, which were further assessed for their binding affinity.

Molecular Docking analyses

To better understand binding interaction of herbal components with p-glycoprotein, molecular docking analysis was performed where verapamil was selected as the control drug. The herbal components (p-glycoprotein inhibitors) were sequentially analysed in order of their best (maximally negative) binding energy viz., thionuphlutine B, kihadanin A, kopsamine, palmatine, bourjotinolone A, guaiaretic acid, richenone, hydnocarpin, cabralealactone, isohydnocarpin, 1,2-benzenedicarboxylic acid, diisooctyl ester/diisooctyl phthalate, guaiacin, stigmasterol, ergosterol acetate, spicatanol, kopsamidine B, matairesinol, proceranone, spicatanol methyl ether and cubebin. The lowest binding energy of interaction was observed to be with thionuphlutine B (-187.15 Kcal/mol), a component present in *N. pumilum*, followed by kihadanin A (-150.85 Kcal/mol) and kopsamine (-126.20 Kcal/mol), components present in *P. amurense* and *K. arborea* respectively **(Figure 1)**.

To analyze the selectivity and strength of the protein-ligand interactions, the hydrogen bonds and hydrophobic interactions were calculated. The analysed inhibitory components in order of their maximum hydrogen bonded interactions were found to be hydnocarpin, cubebin, kopsamine, matairesinol, thionuphlutine B, kihadanin A, isohydnocarpin, kopsamidine B, bourjotinolone A, proceranone, guaiacin, 1,2-benzenedicarboxylic acid, diisooctyl ester/diisooctyl phthalate, spicatanol methyl ether, palmatine, ergosterol acetate, richenone, cabralealactone and guaiaretic acid. Maximal hydrogen bond interactions observed was 04 in hydnocarpin from *H. wightiana.* Thionuphlutine B, a component present in *N. pumilum* displayed two hydrogen bond interactions **(Figure 2)**.

The analysed inhibitory components in order of their maximum hydrophobic interactions were found to be richenone, thionuphlutine B, bourjotinolone A, ergosterol acetate, guaiacin, guaiaretic acid, kopsamine, spicatanol methyl ether, isohydnocarpin, hydnocarpin, spicatanol, proceranone, matairesinol, 1,2-benzenedicarboxylic acid, diisooctyl ester/diisooctyl phthalate, stigmasterol, kopsamidine B, cabralealactone, cubebin, kihadanin A and palmatine. Maximal hydrophobic interaction detected was 09 in richenone from *T. sinensis.* Thionuphlutine B, a component present in *N. pumilum* displayed 8 hydrophobic interactions **(Figure 3)**.

For studying the receptor-ligand binding mechanism, the components were docked with p-glycoprotein by using CDOCKER module of Discovery Studio.

The results revealed that thionuphlutine B, kihadanin A and kopsamine may serve as three best inhibitors of p-glycoprotein. Thionuphlutine B was involved in two hydrogen bond interactions with amino acid residues SER733, GLU972 at distance of 2.67 A° and 2.62 A° respectively and eight hydrophobic (pi-alkyl and alkyl) interactions were detected with amino acid residues PHE79, PHE336, PHE732, LEU332, LEU975, LEU976, ALA729 and ILE736. Similarly, kihadanin A displayed two hydrogen bond interactions with SER733 and GLY737 at distance of 2.44 A° and 2.95 A° respectively and three hydrophobic interactions (pi-alkyl and alkyl) with LEU332, PHE79, ILE736 at distance of 4.60 A°, 3.57 A° and 4.26 A° respectively. Kopsamine showed three hydrogen bond interactions with MET75, THR76, GLU972 at distance of 2.83 A°, 2.31 A° and 2.90 A° respectively and six hydrophobic (pi-pi stacked, pi-alkyl and alkyl) interactions with PHE72, PHE79, ILE328, LEU975, LEU976, ILE736 at a distance of 3.88 A°, 5.15 A°, 5.48 A°, 5.15 A°, 4.51 A° and 5.34 A° respectively **(Figure 4)**. Thionuphlutine B was thus found to be the best compound among the 236 components, primarily based on lowest binding energy, along with maximum hydrogen and hydrophobic interactions with p-glycoprotein. It was thus MD simulated to obtain more detailed and accurate energy values and trajectories to comprehend the binding affinity.

Molecular Dynamics Simulation

To validate the binding mode of the inhibitor and to evaluate the stability of p-glycoprotein-thionuphlutine B complex under dynamic conditions, MD simulation was conducted for 40 ns to acquire the best conformation. RMSD is an important parameter to examine the stability of the complex **(Figure 5)**. There was uniformity in RMSD fluctuation in context of amino acid residue of the protein when p-glycoprotein is bound with the ligand, thionuphlutine B.

Another crucial parameter for determining the complex's stability is its B-factor. It is calculated based on the atomic fluctuations observed during the simulation trajectory. The uniform B-factor graph **(Figure 6)** depicts that stability of the complex is maintained throughout the duration of simulation. The TIPS3BOX solvent model was successfully implemented with a box size of 10 for the p-glycoprotein-thionuphlutine B complex, resulting in a stable B-factor and RMSD graph, indicating that the simulation was successful and the complex was stable.

Clustering

Clustering of small molecules by structural and physicochemical similarities is a powerful approach for correlating structural features of molecules with their

activities. The clustering tree is shown in **Figure 7**. Thionuphlutine B is clustering with a known inhibitor verapamil (control) and other eight molecules, viz., diisooctyl phthalate, hydnocarpin, isohydnocarpin, palmatine, guaiacin, cubebin, matairesinol and guaiaretic acid, which are p-glycoprotein inhibitors. Based on structural similarity and physicochemical properties, thionuphlutine B is similar to this group of molecules.

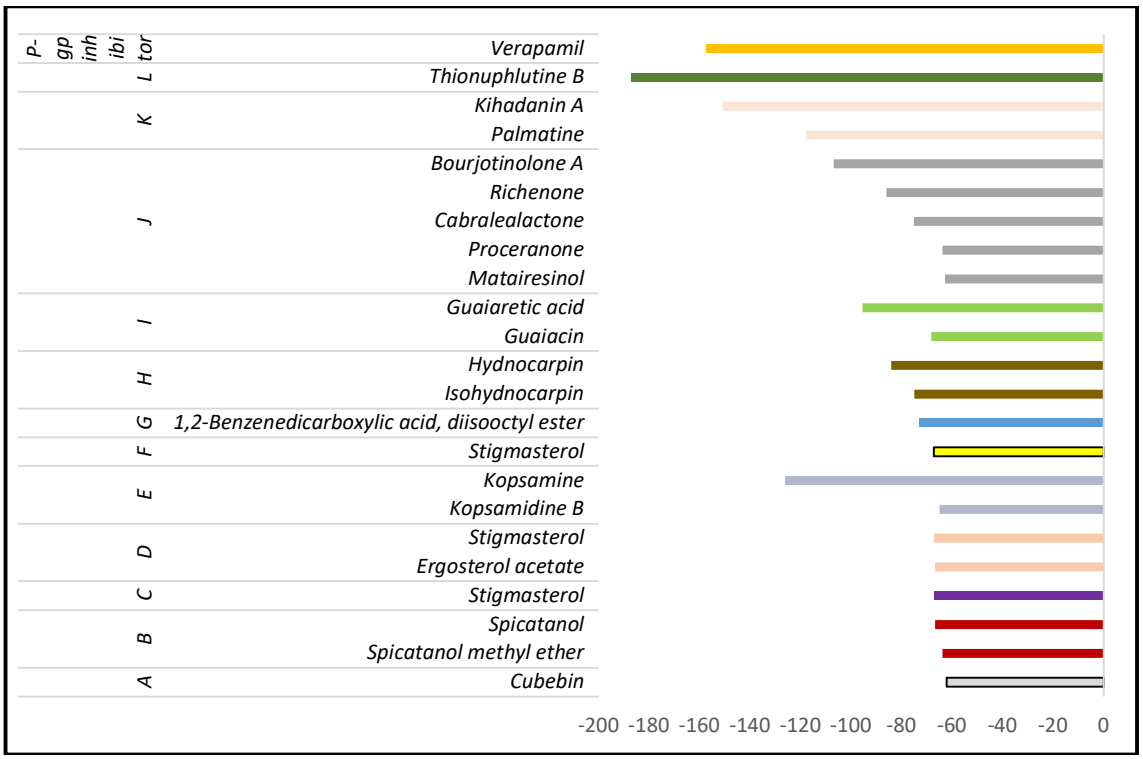

Figure 1: Binding energy of interaction of inhibitory components in antiarthritic herbs viz., *(A) Justicia tranquebariensis; (B) Hedychium spicatum; (C) Cassia fistula; (D) Ficus bengalensis; (E) Kopsia arborea; (F) Artemesia japonica; (G) Hypericum mysorense; (H) Hydnocarpus wightiana; (I) Guaiacum officinale; (J) Toona sinensis; (K) Phellodendron amurense; (L) Nuphar pumilum* **(in sequence of their efficiency) with verapamil as control**

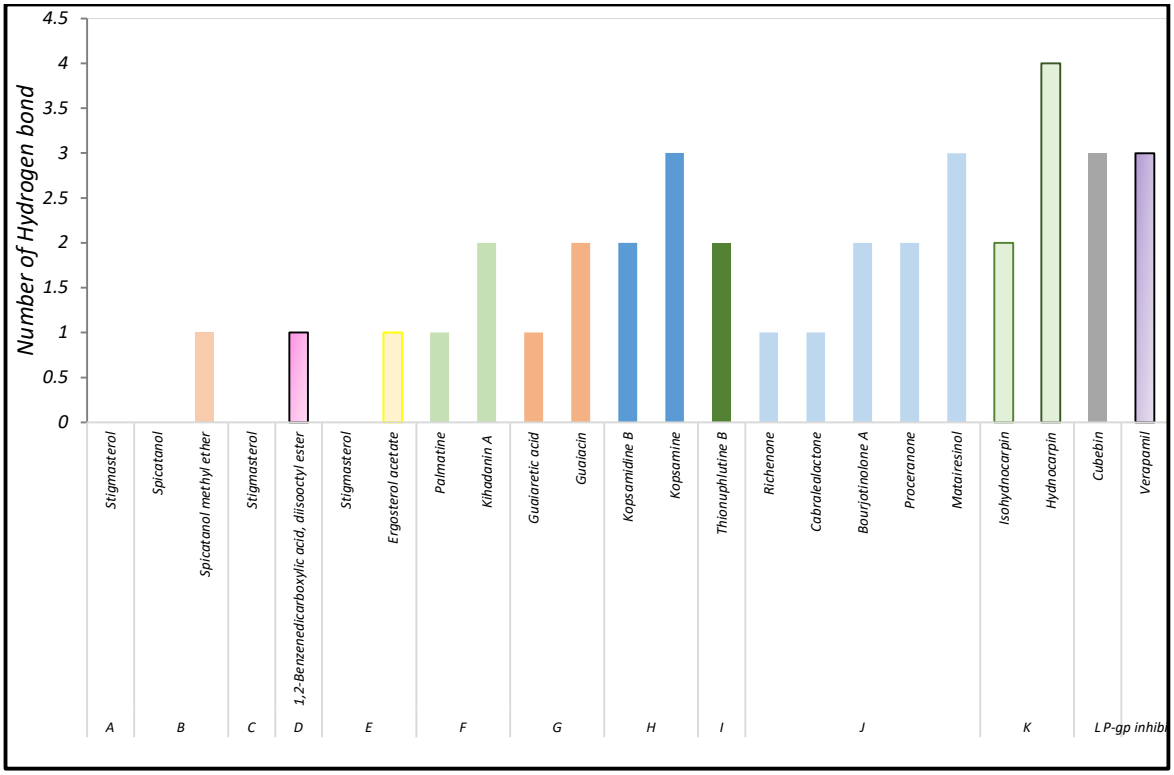

Figure 2: Number of hydrogen bonds of inhibitory components in antiarthritic herbs viz., *(A) Cassia fistula; (B) Hedychium spicatum; (C) Artemesia japonica; (D) Hypericum mysorense; (E) Ficus bengalensis; (F) Phellodendron amurense; (G) Guaiacum officinale; (H) Kopsia arborea; (I) Nuphar pumilum; (J) Toona sinensis; (K) Hydnocarpus wightiana; (L) Justicia tranquebariensis* **(in sequence of their efficiency), where verapamil is considered as the control**

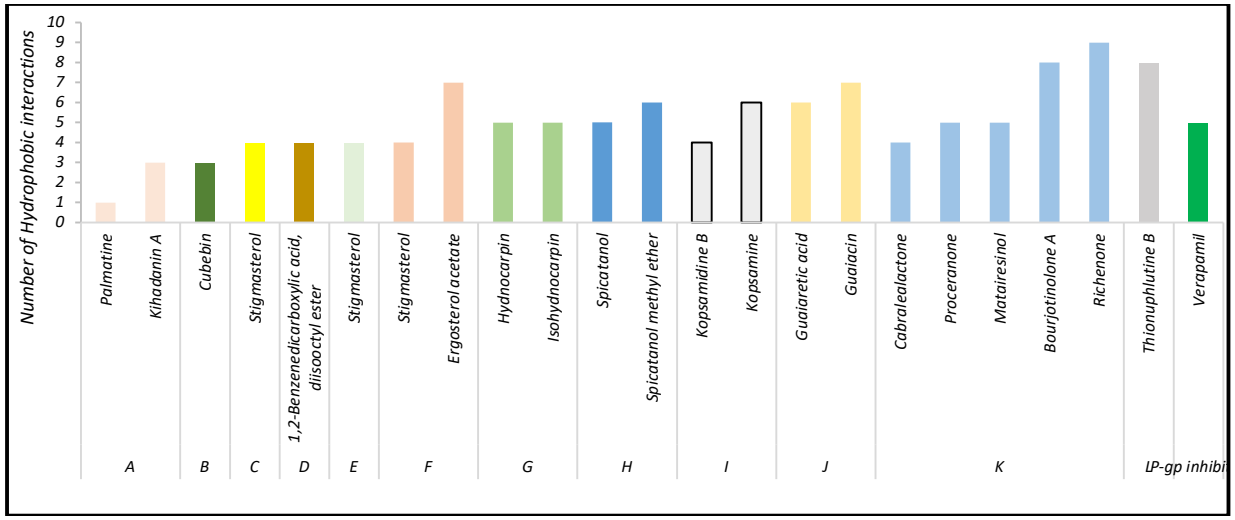

Figure 3: Hydrophobic interactions of inhibitory components in antiarthritic herbs viz., *(A) Phellodendron amurense; (B) Justicia tranquebariensis; (C) Cassia fistula; (D) Hypericum mysorense; (E) Artemesia japonica; (F) Ficus bengalensis; (G) Hydnocarpus wightiana; (H) Hedychium spicatum; (I) Kopsia arborea; (J) Guaiacum officinale; (K) Toona sinensis; (L) Nuphar pumilum* **(in sequence of their efficiency) with verapamil as control**

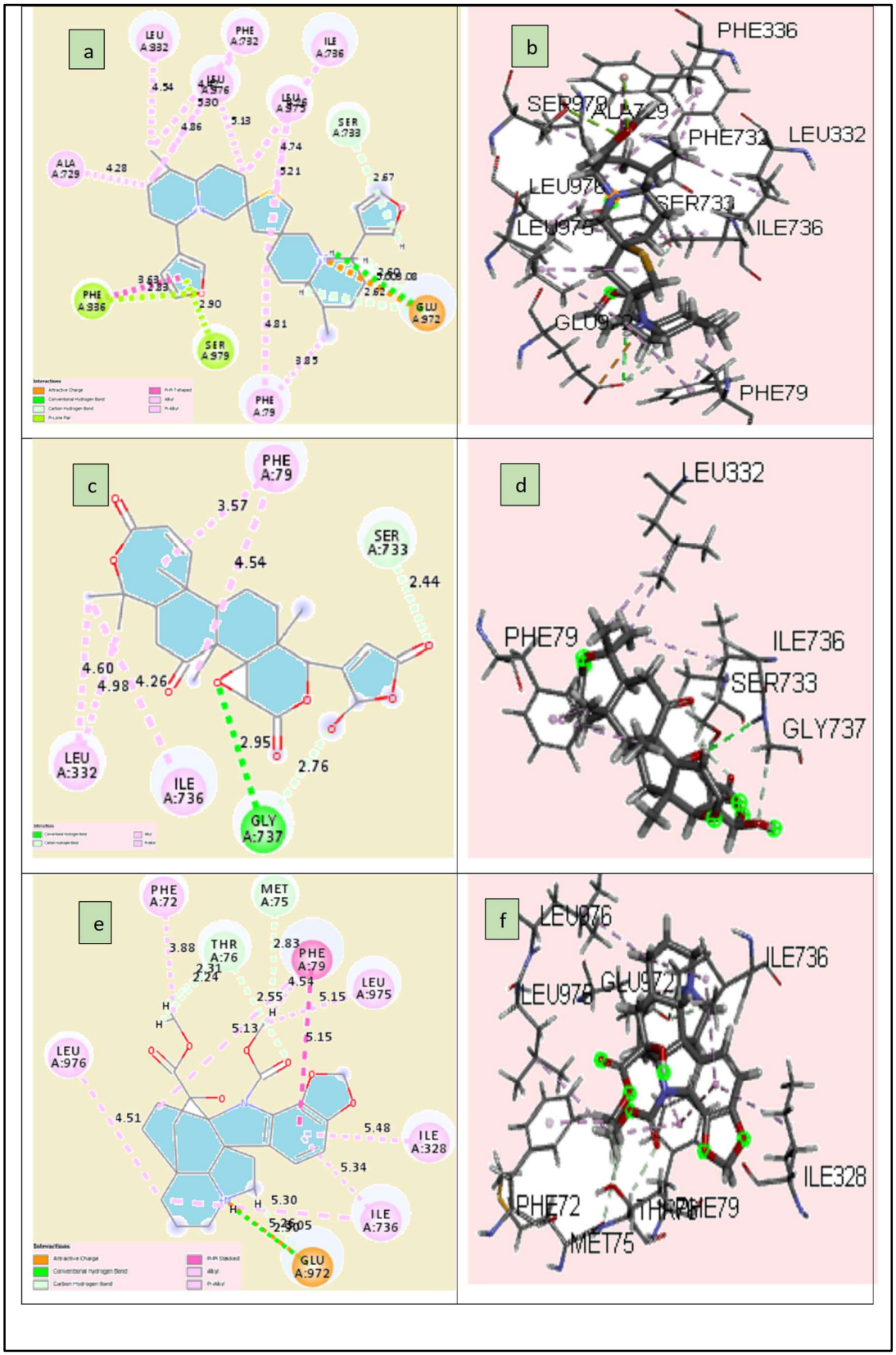

Figure 4: 2D (Left) and 3D (Right) binding poses of inhibitors: (a-b) Thionuphlutine B, (c-d) Kihadanin A and (e-f) Kopsamine with human p-glycoprotein (6C0V). Graphics have been generated by CDOCKER

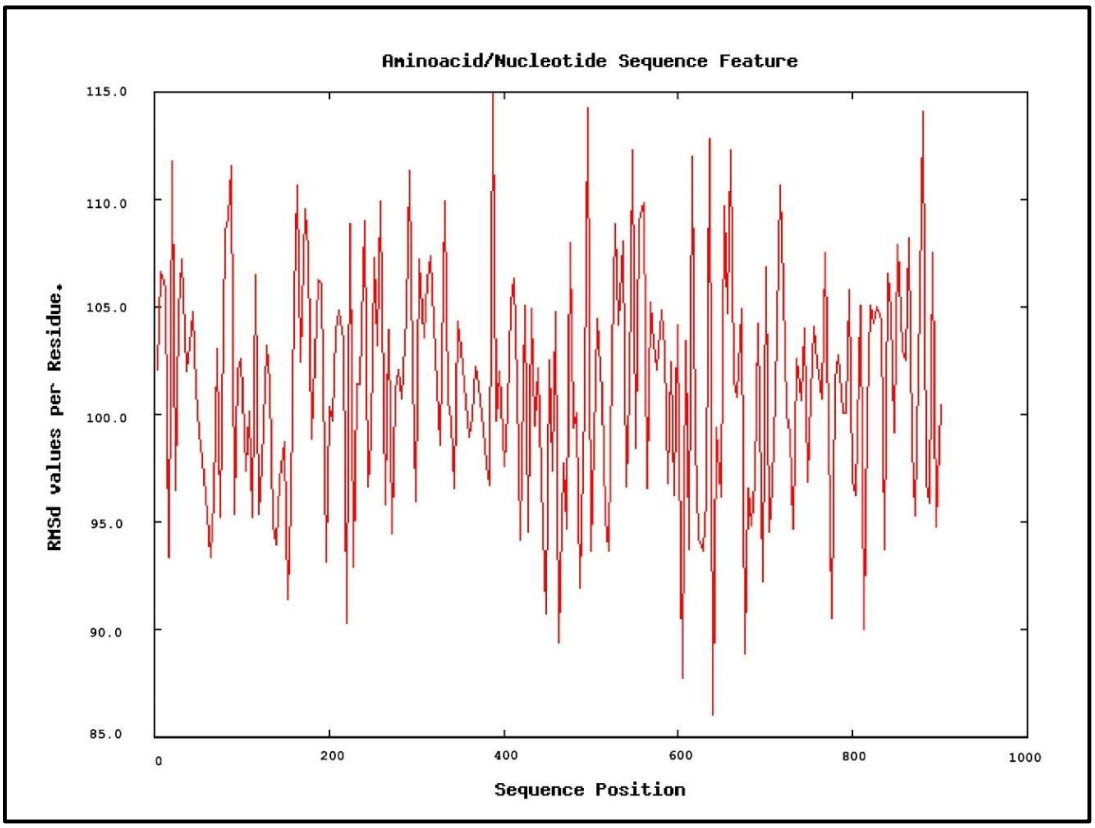

Figure 5: Root Mean Square Deviation curve of p-glycoprotein- thionuphlutine B complex

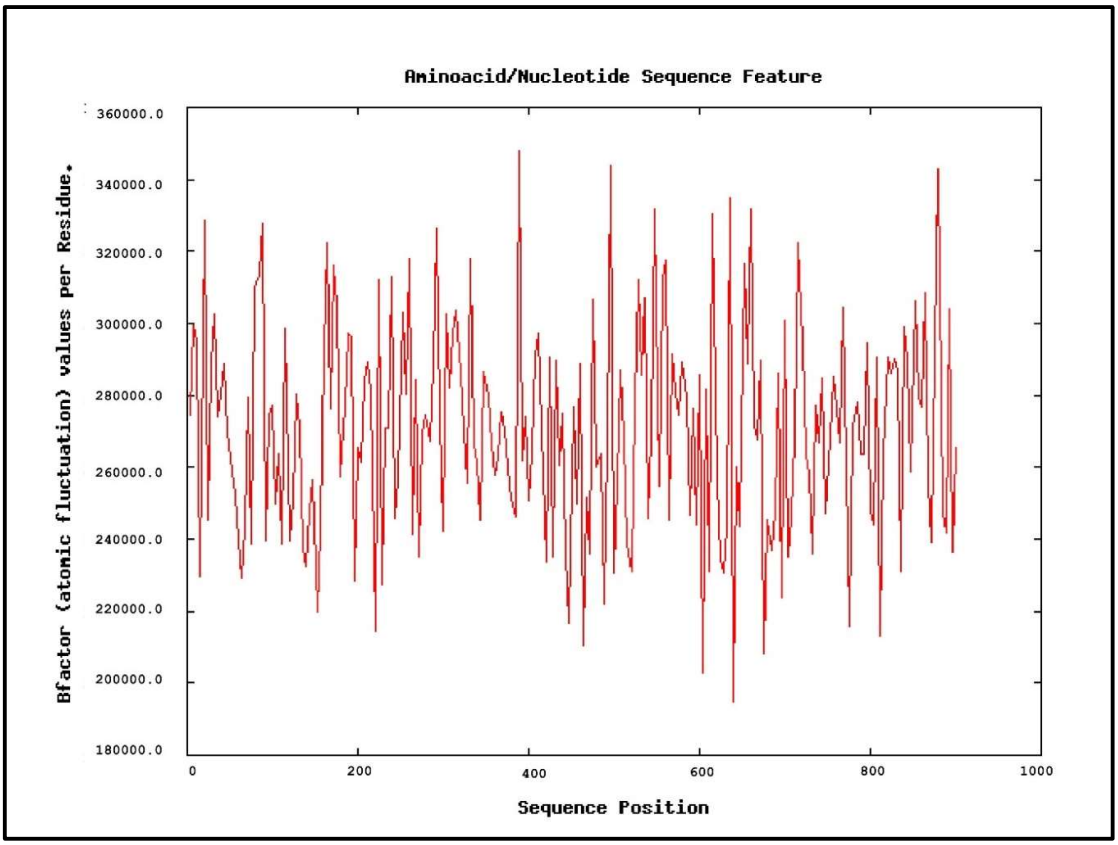

Figure 6: B-factor graph of p-glycoprotein-thionuphlutine B complex

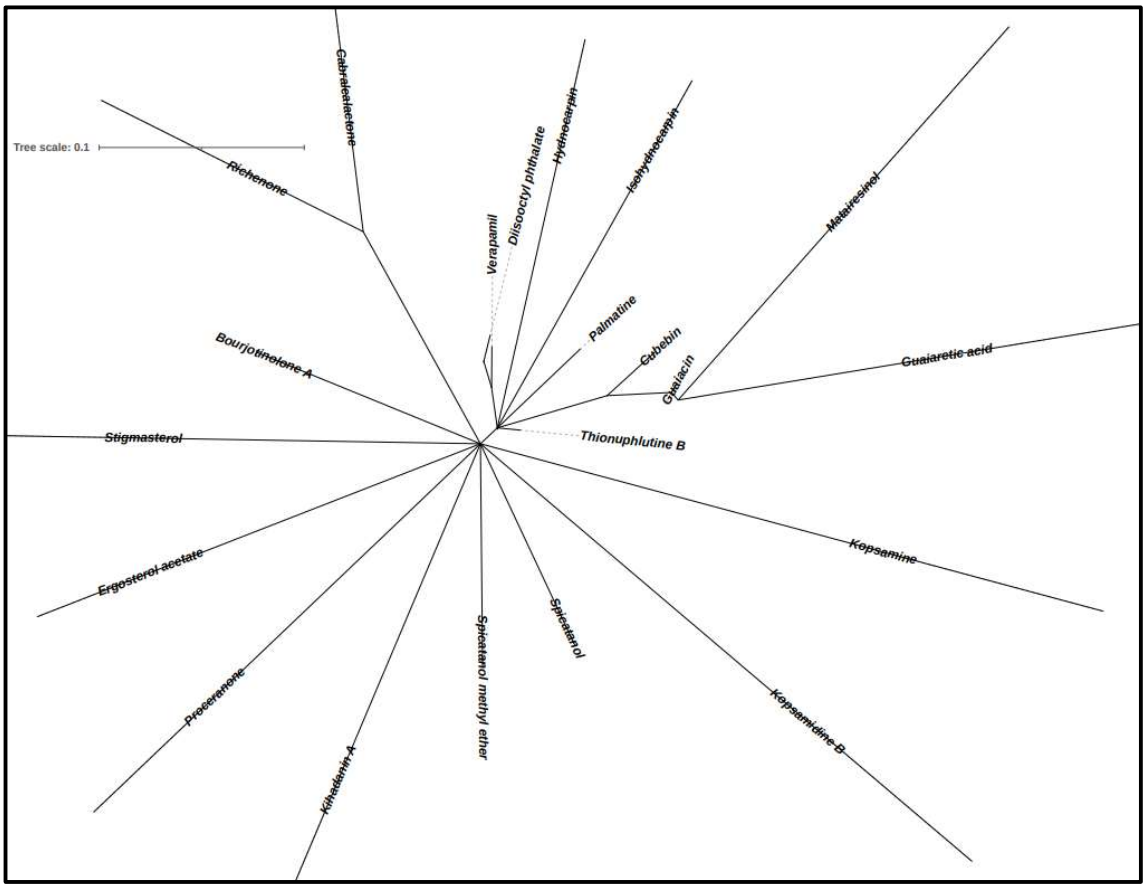

Figure 7: Clustering of p-glycoprotein inhibitors based on structural similarity and physicochemical property calculated by ChemMine software

The present study revealed that thionuphlutine B with its maximum negative binding energy and favourable molecular interactions could likely inhibit p-glycoprotein better than the control drug verapamil and be considered as the lead compound in modulation of p-glycoprotein mediated antiarthritic drug efflux. Additionally, uniformity in RMSD fluctuation and B-factor graph observed during MD simulation revealed that the interaction of p-glycoprotein with thionuphlutine B is stable and hence the desired antiarthritic effect should be imparted. Cluster analysis by physicochemical similarities extended support that thionuphlutine B belongs to the same group of compounds which are known to be inhibitors of p-glycoprotein.

This is hitherto the first work on molecular docking of most of the herbal inhibitors (including thionuphlutine B, kihadanin A and kopsamine) mentioned in this study with 6C0V structure of p-glycoprotein. This is also the first MD simulation study on p-glycoprotein-thionuphlutine B complex. Previous study of molecular docking of p-glycoprotein (6C0V) using AutoDock4.2 program with stigmasterol have shown that it interacts

with binding energy of -8.6 kcal/mol with no hydrogen bond interaction **[40]**. Our docking study using CDOCKER program shows that stigmasterol interacts with 6C0V receptor with binding energy of -67.28 kcal/mol with no hydrogen bond interactions and four hydrophobic interactions.

The docking results further revealed that thionuphlutine B displayed better binding affinity (-187.15 Kcal/mol) than the established inhibitor of p-glycoprotein such as verapamil **[41]** whose binding energy has been determined to be -157.24 Kcal/mol. Verapamil was involved in three hydrogen bond interactions (carbon-hydrogen bond) with amino acid residues LEU332 (bond length 2.36 Å), LEU975 (bond length 2.94 Å) and ILE736 (bond length 2.59 Å). It was engaged in five hydrophobic interactions (one pi-pi T-shaped, one pi-pi stacked and three pi-alkyl) with residues PHE732 (4.46 Å), PHE336 (5.63 Å), PHE79 (4.59 Å), ALA729 (4.90 Å) and ILE736 (5.17Å) respectively. Thionuphlutine B exhibited stronger interactions than verapamil at the same binding position which was evident from two hydrogen bond (conventional and carbon-hydrogen) interactions with amino acid residues SER733 (2.67 A°), GLU972 (2.62 A°) and eight hydrophobic (pi-alkyl, alkyl and pi-pi T-shaped) interactions with residues viz., PHE79 (4.81 Å), PHE732 (4.86 Å), LEU332 (4.54 Å), LEU975 (4.74 Å), LEU976 (5.13 Å), ALA729 (4.28 Å), ILE736 (4.74 Å) and PHE336 (3.63 Å) respectively.

Overcoming p-glycoprotein efflux is an important strategy to improve the bioavailability and pharmacokinetics of its substrate drugs. Increased activity and overexpression of p-glycoprotein leads to development of multidrug resistance, besides changing the pharmacokinetics and pharmacodynamics of these drugs by dictating their ADMET properties **[42]**. Concurrent administration of p-glycoprotein inhibitors along with substrate drugs can overcome the substrate expulsion and render the intended therapeutic benefits in arthritic patients.

Phytochemicals exert synergistic interactions with drugs and overcome resistance via modulation of p-glycoprotein transport through multiple molecular targets and signaling pathways **[43]**. The efficacy of phytochemicals in modulation of p-glycoprotein mediated efflux have been observed in case of silymarin (*S. marianum*) in multidrug resistant human breast cancer MCF-7 cells **[44]**; p-glycoprotein inhibitory activity by kaempferol in Caco-2 cells and multidrug-resistant 1 transfected MDCK cells (*C. fistula*) **[45]**; such inhibition by hydnocarpin in lymphoblastic leukemia cell line (*H. wightiana*) **[46]**; reversal of multidrug resistance in KB CH^R 8-5 cells by quercetin (*T. sinensis*) **[47]**; modulation of

MDR by ferulic acid via inhibition of PI3K/Akt/NF-κB signaling pathway (*A. japonica*) **[48]**. These reflect the role of herbal components in inhibiting p-glycoprotein mediated drug efflux which lowers the drug concentration in the target cell.

Medicinal herbs and their bioactive phytoconstituents interact with numerous drug targets and pathways which make them promising candidate for arthritis treatment. *P. amurense* extract is known to reduce levels of anti-ColII IgG2a antibody, prostaglandin E2, tumor necrosis factor-α (TNF-α) and interleukin-17 in the joints of collagen-induced arthritis in mice **[27]**. Flavonoids viz., quercetin (*T. sinensis*) is found to inhibit cyclooxygenase and lipoxygenase pathways and exhibit antioxidant activity which repress the macrophage phagocytosis in RA **[49]**. Luteolin (*H. wightiana*) and apigenin (*T. parthenium*) lowered the expression of nitric oxide, reactive oxygen species and various cytokines such as TNF-α, IL-6, interferon-γ, and interleukin-2, which is helpful in combating RA **[50, 51]**. Emodin (*C. fistula*) mitigates cartilage inflammation in osteoarthritis by inhibiting nuclear factor-κB and Wnt/β-catenin signaling pathways **[52]**. Kaempferol, a natural flavanol from *T. sinensis* lowered cyclooxygenase 2 level in RAW 264.7 cells, and suppressed reactive oxygen species production through inhibition of inducible nitric oxide synthase and TNF-α expression **[53]**. Deoxynupharidine, an alkaloid isolated from the rhizome of *N. pumilum* has been implicated in the treatment of rheumatoid arthritis through inhibition of synthesis of interleukin-1 and TNF by murine peritoneal macrophages **[17]**. Dimeric sesquiterpene thioalkaloids viz., 6-hydroxythiobinupharidine, 6,6'-dihydroxythiobinupharidine, 6-hydroxythionuphlutine B and quinolizidine alkaloids viz., neothiobinupharidine, nupharidine, deoxynupharidine, 7-epideoxynupharidine and nupharolutine derived from the rhizome of *Nuphar* plant have been observed to exhibit immunosuppressive activity **[54]**. So, antiarthritic herbal components (acting as p-glycoprotein inhibitors), in conjunction with allopathic drugs, would help retain the drug substrate in the cell while enhancing its ameliorative treatment.

CONCLUSION

This study thus delineates the inhibitory capacity of these natural compounds on p-glycoprotein which would allow retention of the antiarthritic drugs that are substrates of the efflux carrier protein. These herbal components promise drug-likeness in addition to ADMET characteristics, suggesting their candidature as potential lead molecules for coadministration with allopathic drugs.

Thionuphlutine B is thus the lead inhibitory compound, followed by kihadanin A and kopsamine, as analyzed from an array of antiarthritic phytocompounds which might play a crucial role in circumvention of p-glycoprotein mediated drug efflux. Further *in vitro* and *in vivo* study may be necessary to authenticate the pharmacological significance of these lead compounds.

ACKNOWLEDGEMENT

We would like to express our heartfelt gratitude to West Bengal State University for providing the infrastructural facilities to pursue our studies.

CONFLICT OF INTEREST

The authors declare that there is no conflict of interest.

REFERENCES

[1] Qin K, Chen K, Zhao W, Zhao X, Luo J, Wang Q, Gao C, Li X, Wang C. Methotrexate combined with 4-hydroperoxycyclophosphamide downregulates multidrug-resistance p-glycoprotein expression induced by methotrexate in rheumatoid arthritis fibroblast-like synoviocytes via the JAK2/STAT3 pathway. Journal of Immunology Research 2018; 18: 3619320. https://doi.org/10.1155/2018/3619320.

[2] Becker JP, Depret G, Van Bambeke F, Tulkens PM, Prévost M. Molecular models of human p-glycoprotein in two different catalytic states. BMC Structural Biology 2009; 9: 3. https://doi.org/10.1186/1472-6807-9-3.

[3] Srivalli KMR, Lakshmi PK. Overview of p-glycoprotein inhibitors: a rational outlook. Brazilian Journal of Pharmaceutical Sciences 2012; 48. https://doi.org/10.1590/S1984-82502012000300002.

[4] Tsujimura S, Saito K, Nawata M, Nakayamada S, Tanaka Y. Overcoming drug resistance induced by p-glycoprotein on lymphocytes in patients with refractory rheumatoid arthritis. Annals of the Rheumatic Diseases 2008; 67: 380–388. https://doi.org/10.1136/ard.2007.070821.

[5] Tsujimura S, Tanaka Y. Disease control by regulation of p-glycoprotein on lymphocytes in patients with rheumatoid arthritis. World Journal of Experimental Medicine 2015; 5(4): 225–231. https://doi.org/10.5493/wjem.v5.i4.225.

[6] Shah FH, Kim SJ. Therapeutic role of medicinal plant extracts and bioactive compounds in osteoarthritis. Advances in

Traditional Medicine 2022. https://doi.org/10.1007/s13596-022-00635-5.

[7] Ganesan M, Kanimozhi G, Pradhapsingh B, Khan HA, Alhomida AS, Ekhzaimy A, Brindha GR, Prasad NR. Phytochemicals reverse p-glycoprotein mediated multidrug resistance via signal transduction pathways. Biomedicine and Pharmacotherapy 2021; 139: 111632. https://doi.org/10.1016/j.biopha.2021.111632.

[8] Posada MM, Cannady EA, Payne CD, Zhang X, Bacon JA, Pak YA, Higgins JW, Shahri N, Hall SD, Hillgren KM. Prediction of transporter-mediated drug-drug interactions for baricitinib. Clinical and Translational Science 2017; 10: 509–519. https://doi.org/10.1111/cts.12486.

[9] Fu R, Wang XN, Guo CH, Li Y, Ding CY, Li YJ, Dong ZJ. Wuzhi capsule increased systemic exposure to methotrexate by inhibiting the expression of OAT1/3 and p-gp. Annals of Translational Medicine 2021 ; 9(10): 845.

[10] Dilger K, Schwab M, Fromm MF. Identification of budesonide and prednisone as substrates of the intestinal drug efflux pump p-glycoprotein. Inflammatory Bowel Diseases 2004; 10(5): 578–583. https://doi.org/10.1097/00054725-200409000-00012.

[11] Zerilli T, Ocheretyaner E. Apremilast (otezla): a new oral treatment for adults with psoriasis and psoriatic arthritis. Pharmacy and Therapeutics 2015; 40: 495–500.

[12] Gwak EH, Yoo HY, Kim SH. Effects of diabetes mellitus on the disposition of tofacitinib, a janus kinase inhibitor in rats. Biomolecules and Therapeutics 2020; 28(4): 361–369. https://doi.org/10.4062/biomolther.2020.006.

[13] Anglicheau D, Pallet N, Rabant M, Marquet P, Cassinat B, Méria P, Beaune P, Legendre C, Thervet E. Role of p-glycoprotein in cyclosporine cytotoxicity in the cyclosporine-sirolimus interaction. Kidney International 2006; 70(6): 1019–1025. https://doi.org/10.1038/sj.ki.5001649.

[14] Mohamed MF, Klünder B, Othman AA. Clinical pharmacokinetics of upadacitinib: review of data relevant to the rheumatoid arthritis indication. Clinical

Pharmacokinetics 2020; 59(5): 531–544. https://doi.org/10.1007/s40262-019-00855-0.

[15] Choudhary M, Kumar V, Malhotra H, Singh S. Medicinal plants with potential anti-arthritic activity. Journal of Intercultural Ethnopharmacology 2015; 4(2): 147–179. https://doi.org/10.5455/jice.20150313021918.

[16] Li Ning, Shi Chenchen, Shi Songshan, Wang Huijun, Yan Jun. An inulin-type fructan isolated from *Artemisia japonica* and its antiarthritic effects. Journal of Functional Foods 2017; 29: 29-36. https://doi.org/10.1016/j.jff.2016.11.033.

[17] Zhang L, Huang Y, Qian Y, Xiao P. Effect of deoxynupharidine on immune function *in vitro*. Acta Academiae Medicinae Sinicae 1995; 17: 343-348.

[18] Sivasamy G, Senthil D, Ramachandran G, Palaniswamy R. Review on characteristics of *Justicia tranquebariensis.* International Journal of Creative Research Thoughts 2021; 9.

[19] Gopinath S, Sakthidevi G, Muthukumaraswamy S, Mohan VR. GC-MS analysis of bioactive constituents of *Hypericum mysorense* (Hypericaceae). Journal of Chemical and Pharmaceutical Sciences 2013; 3: 6-15.

[20] Jabbari M, Daneshfard B, Emtiazy M, Khiveh A, Hashempur MH. Biological effects and clinical applications of dwarf elder (*Sambucus ebulus* L): A Review. Journal of evidence-based complementary and alternative medicine 2017; 22: 996–1001.

[21] Shang CH, Zhang QQ, Zhou JH. Oridonin inhibits cell proliferation and induces apoptosis in rheumatoid arthritis fibroblast-like synoviocytes. Inflammation 2016; 39: 873–880. https://doi.org/10.1007/s10753-016-0318-2.

[22] Pareek A, Suthar M, Rathore GS, Bansal V. Feverfew (*Tanacetum parthenium* L.): A systematic review. Pharmacognosy Reviews 2011; 5: 103–110.

[23] Han L, Zhou X, Yang M, Zhou L, Deng X, Wei S, Wang W, Wang Z, Qiao X, Bai C. Ethnobotany, phytochemistry and pharmacological effects of plants in genus *Cynanchum* Linn. (Asclepiadaceae). Molecules 2018; 23: 1194.

https://doi.org/10.3390/molecules23051194.

[24] Zhang W, Li R, Wang S, Mu F, Jia P. Effect of Chinese traditional herb *Epimedium grandiflorum* C. morren and its extract icariin on osteoarthritis via suppressing NF-kappaB pathway. Indian Journal of Experimental Biology 2013; 51: 313-321.

[25] Gupta OP, Sing S, Bani S, Sharma N, Malhotra S, Gupta BD, Banerjee SK, Handa SS. Anti-inflammatory and antiarthritic activities of silymarin acting through inhibition of 5-lipoxygenase. Phytomedicine 2000; 7: 21–24. https://doi.org/10.1016/S0944-7113(00)80017-3.

[26] Kitajimaa M, Koyamaa T, Wua Y, Kogurea N, Zhangb R, Takayamaa H. Kopsiyunnanines J1 and J2, new strychnos-type homo-monoterpenoid indole alkaloids from *Kopsia arborea*. Natural Product Communications 2015; 10.

[27] Jung HW, Kim KH, Park YK. Inhibitory effect of the extract of Phellodendron amurense ruprecht root on collagen-induced arthritis in mice. Chinese Journal of Integrative Medicine 2017; 23: 755-762.

[28] Yang YL, Chen C. Effects of total polyphenols from seeds of Toona sinensis in treating adjuvant-induced arthritis rats. Chinese Journal of Modern Applied Pharmacy 2012; 29: 1073–1077.

[29] Moloudizargari M, Mikaili P, Aghajanshakeri S, Asghari MH, Shayegh J. Pharmacological and therapeutic effects of *Peganum harmala* and its main alkaloids. Pharmacognosy Reviews 2013; 7: 199–12.

[30] Petchi RP, Vijaya C. Anti-diabetic and antiarthritic potential of *Glycosmis pentaphylla* stem bark in FCA induced arthritis and streptozotocin induced diabetic rats. International Journal of Pharma and Bio Sciences 2012; 3: P328-P36.

[31] Sravani T, Paarakh PM. *Hedychium spicatum* Buch. Ham. - an overview. Pharmacologyonline Newsletter 2011; 2: 633-42.

[32] Kim Y, Chen J. Molecular structure of human p-glycoprotein in the ATP-bound, outward-facing conformation. Science 2018; 359: 915-919. https://doi.org/10.1126/science.aar7389.

[33] Alder BJ, Wainwright TE. Studies in molecular dynamics. I. General

method. The Journal of Chemical Physics 1959; 31: 459-466.

[34] Ding F, Buldyrev SV, Dokholyan NV. Folding Trp-cage to NMR resolution native structure using a coarse-grained protein model. Biophysical Journal 2005; 88: 147-155. https://doi.org/10.1529/biophysj.104.046375.

[35] Marchut AJ, Hall CK. Side-chain interactions determine amyloid formation by model polyglutamine peptides in molecular dynamics simulations. Biophysical Journal 2006; 90: 4574-4584. https://doi.org/10.1529/biophysj.105.079269.

[36] Nguyen HD, Hall CK. Molecular dynamics simulations of spontaneous fibril formation by random-coil peptides. Proceedings of the National Academy of Sciences 2004; 101: 16180-16185. https://doi.org/10.1073/pnas.0407273101.

[37] Nguyen HD, Reddy VS, Brooks CL. Deciphering the kinetic mechanism of spontaneous self-assembly of icosahedral capsids. Nano Letters 2007; 7: 338-344. https://doi.org/10.1021/nl062449h.

[38] Kovacs JA, Chacon P, Abagyan R. Predictions of protein flexibility : first-order measures. Proteins 2004; 56: 661-668. https://doi.org/10.1002/prot.20151.

[39] Backman TW, Cao Y, Girke T. ChemMine tools: an online service for analyzing and clustering small molecules. Nucleic Acids Research 2011; 39 (Web Server issue): W486–W491. https://doi.org/10.1093/nar/gkr320 .

[40] Yalcin S. Molecular Docking, Drug Likeness, and ADMET Analyses of Passiflora compounds as P-glycoprotein (P-gp) inhibitor for the treatment of cancer. Current Pharmacology Reports 2020; 6: 429-440.

[41] Bansal T, Mishra G, Jaggi M, Khar RK, Talegaonkar S. Effect of p-glycoprotein inhibitor, verapamil, on oral bioavailability and pharmacokinetics of irinotecan in rats. European Journal of Pharmaceutical Sciences 2009; 36: 580-590. https://doi.org/10.1016/j.ejps.2008.12.005.

[42] Lin JH. Drug-drug interaction mediated by inhibition and induction of p-glycoprotein. Advanced Drug Delivery Reviews 2003; 55: 53-81.

https://doi.org/10.1016/s0169-409x(02)00171-0.

[43] Tinoush B, Shirdel I, Wink M. Phytochemicals: potential lead molecules for mdr reversal. Frontiers in Pharmacology 2020; 11: 832. https://doi.org/10.3389/fphar.2020.00832.

[44] Abdallah HM, Al-Abd AM, El-Dine RS, El-Halawany AM. P-glycoprotein inhibitors of natural origin as potential tumor chemo-sensitizers: a review. Journal of Advanced Research 2015; 6: 45–62. https://doi.org/10.1016/j.jare.2014.11.008.

[45] Patel J, Buddha B, Dey S, Pal D, Mitra AK. *In vitro* interaction of the HIV protease inhibitor ritonavir with herbal constituents: changes in p-gp and CYP3A4 activity. American Journal of Therapeutics 2004; 11: 262-277. https://doi.org/10.1097/01.mjt.0000101827.94820.22.

[46] Pérez LB, Pan Li, Sass E, Gupta SV, Lehman A, Kinghorn AD, Lucas DM. Potentiating effect of the flavonolignan (-)-hydnocarpin in combination with vincristine in a sensitive and p-gp-expressing acute lymphoblastic leukemia cell line. Phytotherapy Research 2013; 27. https://doi.org/10.1002/ptr.4903.

[47] Mohana S, Ganesan M, Agilan B, Karthikeyan R, Srithar G, Beaulah MR, Ananthakrishnan D, Velmurugan D, Rajendra PN, Ambudkar SV. Screening dietary flavonoids for the reversal of p-glycoprotein-mediated multidrug resistance in cancer. Molecular BioSystems 2016; 12: 2458–2470. https://doi.org/10.1039/c6mb00187d.

[48] Muthusamy G, Gunaseelan S, Prasad NR. Ferulic acid reverses p-glycoprotein mediated multidrug resistance via inhibition of PI3K/Akt/NF-κB signaling pathway. Journal of Nutritional Biochemistry 2019; 63: 62-71. https://doi.org/10.1016/j.jnutbio.2018.09.022.

[49] Guardia T, Rotelli AE, Juarez AO, Pelzer LE. Anti-inflammatory properties of plant flavonoids. Effects of rutin, quercetin and hesperidin on adjuvant arthritis in rat. Farmaco 2001; 56: 683-687. https://doi.org/10.1016/s0014-827x(01)01111-9.

[50] Jiang CP, He X, Yang XL, Zhang SL, Li H, Song ZJ, Zhang CF, Yang ZL, Li P, Wang CZ, Yuan CS. Anti-rheumatoid arthritis

activity of flavonoids from *Daphne genkwa*. Phytomedicine 2014; 21: 830–837. https://doi.org/10.1016/j.phymed.2014.01.009.

[51] Sun YW, Bao Y, Yu H, Chen QJ, Lu F, Zhai S, Zhang CF, Li F, Wang CZ, Yuan CS. Anti-rheumatoid arthritis effects of flavonoids from *Daphne genkwa*. International Immunopharmacology 2020; 83. https://doi.org/10.1016/j.intimp.2020.106384.

[52] Ding QH, Ye CY, Chen EM, Zhang W, Wang XH. Emodin ameliorates cartilage degradation in osteoarthritis by inhibiting NF-kappaB and Wnt/beta-catenin signaling *in vitro* and *in vivo*. International Immunopharmacology 2018; 61: 222–230. https://doi.org/10.1016/j.intimp.2018.05.026.

[53] Jain S, Vaidya A, Gupta PK, Rosenholm JM, Bansal KK. Antiarthritic activities of herbal isolates: a comprehensive review. Coatings 2021; 11: 1329. https://doi.org/10.3390/coatings11111329.

[54] Qin J, Wang W, Zhang R. Novel natural product therapeutics targeting both inflammation and cancer. Chinese Journal of Natural Medicines 2017; 15: 401-416. https://doi.org/10.1016/S1875-5364(17)30062-6.